DOI: 10.2118/200581-PA Date: 14-October-20 Stage: Page: 1 Total Pages: 18

A Multisolution Optimization Framework for Well Placement and Control

Mohammad Salehian, Morteza Haghighat Sefat, and **Khafiz Muradov,** Heriot-Watt University

Summary

Field development and control optimization aim to maximize the economic profit of oil and gas production. Mathematically, this results in a complex optimization problem with a large number of correlated decision (also known as control) variables of various types at different levels (e.g., at the level of well location variables or at the level of well production/injection control also know as well control or control settings variables) and a computationally expensive objective function (i.e., a reservoir simulation model). Current multilevel optimization frameworks provide only a single optimal scenario for a field development and control problem. However, unexpected problems that commonly arise during field development and operations can impose extra constraints, resulting in operators having to eventually select an adjusted, and most-likely, nonoptimal scenario.

This work proposes a novel multisolution optimization framework, based on sequential optimization of control variables at multiple levels, providing the flexibility for operators to make optimal decisions while considering operational constraints. An ensemble of close-to-optimum solutions is selected from each level (e.g., from the well location optimization level) and transferred to the next level of optimization (e.g., to the control settings optimization), and this loop continues until no significant improvement is observed in the objective value. Fit-for-purpose clustering techniques are also developed to systematically select an ensemble of solutions, with maximum differences in well locations and control settings but small variation in the objective values, at each level of the optimization.

The developed framework has been tested on two benchmark case studies. The results demonstrate high economic and operational efficiency of the developed multisolution framework as compared to the traditional approaches that rely on single-solution optimization. It is shown that suboptimal solutions from an early optimization level could approach the optimal solution at the next level(s), highlighting the value of the developed multisolution framework to deliver operational flexibility by a more efficient exploration of the search space.

Introduction

Well location and control settings are critical decisions that need to be made during field development and production optimization studies in order to maximize the economic profit of oil and gas production. Several efforts have been made to develop efficient frameworks to optimize the system with one or multiple types of such decision variables. There is no unique terminology for referring to individual subproblems with different types of decision variables. Li et al. (2013) described the optimization of multiple types of variables as "coupled" optimization, while decision variables of different type are optimized in "subproblems." Lu et al. (2017a) used the term "iterative" optimization for referring to optimization problems with decision variables of different types. In this paper, we refer to optimization on different variable types as different levels (e.g., the well location optimization is one level, and the well production/injection control optimization is another level).

Single-level optimization workflows were initially developed to optimize variables at a particular level only, such as well locations (Wang et al. 2012; Awotunde and Naranjo 2014; Al-Ismael et al. 2018) or control settings (Wang et al. 2002; Li and Reynolds 2011; Haghighat Sefat 2016; Lu et al. 2017b; Wang et al. 2019). These were later extended to multilevel optimization, aiming to achieve an optimal solution considering multiple levels altogether (e.g., optimizing the drilling order, well type, location, and control settings) and taking into account the interdependence between them during the optimization process (Li et al. 2013; Tavallali et al. 2013; Forouzanfar et al. 2016; Shirangi et al. 2018). The multilevel optimization frameworks published to date can be classified as:

Joint optimization (Li et al. 2013; Tavallali et al. 2013; Isebor et al. 2014; Shirangi et al. 2018): This approach simultaneously optimizes a single augmented vector of all the control variables from all levels (e.g., all well locations and control settings). This, however, could result in optimization algorithm failure due to its being unable to cope with a large number of control variables (Lu et al. 2017a).

Sequential optimization (Li and Jafarpour 2012; Forouzanfar et al. 2016; Lu et al. 2017a): Techniques have been developed to reduce the number of control variables by dividing the main problem into subproblems, in which each subproblem contains single-type control variables related to an individual optimization level. The field design is iteratively optimized as a sequence of such subproblems (in order to capture a correlation between the values of control variables in optimal scenarios), and the loop is terminated when no major improvement is observed in the objective value (Li and Jafarpour 2012). Lu et al. (2017a) compared the iterative sequential method with the joint method in the context of well placement and control optimization while using an approximate-gradient-based algorithm. Better performance was achieved using the iterative sequential approach, mainly due to the lower quality of the gradient in the joint method with a single augmented vector of control variables of different types (i.e., discrete well locations and continuous control settings).

Both the gradient-based and the derivative-free algorithms have been used in field development and production control optimization studies. The adjoint-gradient- based method has been shown to be computationally fast (Sarma et al. 2005; Kraaijevanger et al. 2007; Bukshtynov et al. 2015) and has been employed in field development studies using in-house reservoir simulators (Brouwer and Jansen 2002; Sarma et al. 2005; Van Essen et al. 2011). However, calculation of the adjoint gradient requires access to the subsurface flow simulation source code; hence, this approach cannot be easily used with many commercial reservoir flow simulators. Alternative algorithms

Original SPE manuscript received for review 16 June 2020. Revised manuscript received for review 17 September 2020. Paper (SPE 200581) peer approved 24 September 2020.

have been developed, which use an estimation of the gradient calculated using black-box simulators, to iteratively move along the control variables in the approximately optimum direction (Sefat et al. 2016; Lu et al. 2017b). The estimated gradient is approximately calculated using an ensemble of simultaneous perturbations of the control variables. Such algorithms include simultaneous perturbation stochastic approximation (SPSA) (Spall 1998) and different variations of ensemble-based optimization (Chen et al. 2009), such as the stochastic simplex approximate gradient (StoSAG) method (Fonseca et al. 2017). SPSA has been used in well placement (Li et al. 2013; Bangerth et al. 2006) and control settings (Sefat et al. 2016) optimization problems, showing its efficiency in handling a large number of variables. StoSAG has been also successfully employed in well control problems (Lu et al. 2017a, b) and has been shown to outperform the classic ensemble-based optimization, developed by Chen et al. (2009) in large-scale robust optimization problems (Lu et al. 2017b). Gradient-based methods can provide computational advantages in terms of efficiency. They, however, have issues with handling categorical (e.g., well-type) variables. Derivative-free optimization methods have also been used in the context of field development and control. These include particle swarm optimization (Eberhart and Kennedy 1995; Ciaurri et al. 2011; Isebor et al. 2014) and genetic algorithms (Holland 1992; Stoisits et al. 2001; Almeida et al. 2010). These methods can handle all types of variables (e.g., categorical, integer, continuous). However, they typically require many more function evaluations than gradient-based algorithms (Tsou and MacNish 2003; Zingg et al. 2008). Application examples of these approaches are described by Stoisits et al. (2001), Almeida et al. (2010), Onwunalu and Durlofsky (2010), Ciaurri et al. (2011), Panahli (2017), Tavallali et al. (2018), and Lu and Reynolds (2019).

This work investigates field development and control optimization in a relatively large-scale problem by employing a sequential optimization approach. One of the limitations of the available, published sequential frameworks is that only a single optimal solution is provided as the output **(Fig. 1a)**. However, unexpected issues that commonly arise during field development and operation can impose extra constraints, resulting in operators having to come up with an adjusted, no longer optimal scenario. For instance, the well location solution provided by the optimization algorithm may appear impractical or difficult to drill as a result of deviation of the actual well trajectory from the planned one. This necessitates the development of a multisolution framework to provide the much-needed operational flexibility to field operators. Previous works (Fonseca et al. 2014; Haghighat Sefat 2016) showed that the search space in the field development optimization problems with a large number of control variables contains several local optima regions whose objective function values are similar. Therefore, an efficient optimization framework can explore the search space to identify multiple solutions with distinctly different values of the control variables but still with the close-to-optimum objective values. The developed framework in this study is based on the iterative sequential approach. Therefore, similar conclusions as Lu et al. (2017a) are valid for this framework, providing greater optimization performance than both joint and sequential approaches. Moreover, the developed multisolution framework provides greater exploration of the search space as well as operational flexibility, in which an ensemble of optimal solutions with close to optimum objective function values and distinctly different values of control variables are transferred between optimization levels (subproblems), as shown in Fig. 1b. Fit-for-purpose clustering techniques are developed to systematically select an ensemble of solutions from each subproblem. SPSA is employed as the optimization algorithm in this work; however, the developed framework is compatible with other optimization algorithms.

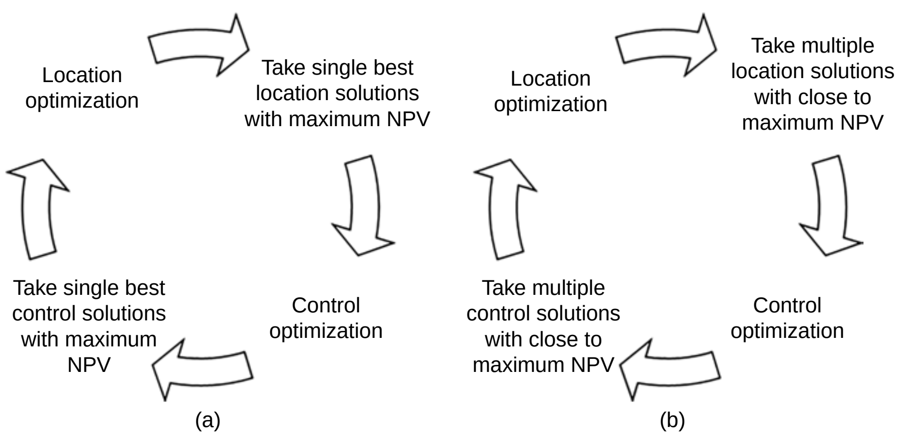

Fig. 1—(a) The existing single solution optimization framework for well placement and control. (b) The developed multisolution optimization framework for well placement and control.

The outline of this paper is as follows: First, problem formulation for multilevel optimization of well placement and control and details of the SPSA algorithm are presented. Then, the structure of the developed multisolution optimization framework is explained followed by its application to two benchmark case studies (Brugge and Egg model). Finally, the results are presented, and the conclusions are drawn.

Problem Formulation in Multilevel Optimization

The objective is to maximize the net present value (NPV) over the presumed production life of the reservoir. Given that we fix the number of wells to drill, each solution has roughly the same capital expenditure (i.e., CAPEX or investment); hence the incremental NPV used to compare solutions in this study only considers cash flow due to oil and water production as follows:

$$J(x,m) = \sum_{n=1}^{S} \left\{ \left[\sum_{j=1}^{N_P} \left(r_o q_{o,j}^n - r_{pw} q_{w,j}^n \right) - \sum_{k=1}^{N_I} \left(c_{wi} q_{wi,k}^n \right) \right] \times \frac{\delta t^n}{(1+b)^{t_n}} \right\}, \quad (1)$$

where x is the N_x dimensional vector of the optimization variables; m is the N_m dimensional state vector of the reservoir (e.g., saturation, pressure field); n is the nth timestep of the reservoir simulation; S is the total number of simulation steps; δt^n is the length of nth

simulation step; t_n is the simulation time at the end of the nth timestep; the annual discount rate b is in decimal; and N_P and N_I are the number of producers and injectors, respectively. The cost coefficients r_o, r_{pw}, and c_{wi} are the oil price (USD/STB), the water handling cost (USD/STB), and the water injection cost (USD/STB), respectively. $q^n_{o,j}$ and $q^n_{w,j}$ are the oil and water production rates of well j at timestep n in STB/day. $q^n_{wi,k}$ is the water injection rate of well k at timestep n in STB/day. The production forecast simulation model is run using a commercial reservoir simulator (ECLIPSE-100) (Schlumberger 2017). This study focuses on the development of the optimization framework; hence, only a single set of reservoir model state parameters (i.e., a single model realization) is considered. In this study, Eq. 2 is employed to scale the control variables x from the domain $[x_{min}, x_{max}]$ to [0, 1] to eliminate the problem of different types of control variables with different ranges at various optimization levels.

$$u_i = \frac{x_i - x_{min,i}}{x_{max,i} - x_{min,i}}. \quad \ldots\ldots (2)$$

Simultaneous Perturbation Stochastic Approximation (SPSA)

SPSA is a stochastic optimization algorithm that approximates the steepest descent (or ascent) gradient with a randomly selected stencil (Spall 1992). Consider $J(x_k)$ to be the objective value based on x_k, the N_x dimensional vector of the control variables at iteration k. The steepest descent gradient $g_k(x)$ is defined as the partial derivatives of the objective function $g_k(x) = \frac{\partial J}{\partial x} = \left[\frac{\partial J}{\partial x_1}, \frac{\partial J}{\partial x_2}, \ldots, \frac{\partial J}{\partial x_{N_x}}\right]^T$, where $[.]^T$ represents a column vector. SPSA iteratively maximizes the objective function $J(x)$ using the following relationship:

$$x_{k+1} = x_k + \alpha_k \hat{g}_k(x_k), \quad \ldots\ldots (3)$$

where $\hat{g}_k(x_k)$ is the stochastically estimated gradient of the objective function and $\alpha_k > 0$ is the step size in the search direction $\hat{g}_k(x_k)$. In order to calculate $\hat{g}_k(x_k)$ Δ_k is defined as a vector of mutually independent, mean-zero random variables $\{\Delta_{k_1}, \Delta_{k_2}, \ldots, \Delta_{k_{N_x}}\}$ using symmetric ± 1 Bernoulli distribution (Spall 1992), meeting the following conditions:

$$\Delta_{k_i}^{-1} = \Delta_{k_i} \quad \ldots\ldots (4)$$

$$E|\Delta_{k_i}^{-1}| = E|\Delta_{k_i}| = 0. \quad \ldots\ldots (5)$$

Here, E represents the expected value. The stochastic gradient $\hat{g}_k(x_k)$ is calculated using Δ_k and a positive scalar c_k:

$$\hat{g}_k(x_k) = \frac{J(x_k + c_k\Delta_k) - J(x_k - c_k\Delta_k)}{2c_k} \times \left[\frac{1}{\Delta_{k_1}}, \frac{1}{\Delta_{k_2}}, \ldots, \frac{1}{\Delta_{k_{N_x}}}\right]^T. \quad \ldots\ldots (6)$$

The convergence of the SPSA algorithm relies on the tuning parameters α_k and c_k, which are particularly important when objective function is computationally expensive. Spall (1998) suggested the following decaying sequences to calculate α_k and c_k to ensure a gradually refining search:

$$\alpha_k = \frac{a}{(\mathbb{A} + k + 1)^{\vartheta}} \quad \ldots\ldots (7)$$

$$c_k = \frac{c}{(k+1)^{\gamma}}, \quad \ldots\ldots (8)$$

where a, c, $\mathbb{A}$, ϑ, and γ are positive real numbers. The stability constant $\mathbb{A}$ is recommended to be 5 to 10% of the expected, or allowed, number of iterations. Sefat et al. (2016) investigated the optimal tuning parameters values in the context of well control optimization and recommended the proposed values of 0.602 and 0.101 for ϑ and γ, respectively, while defining $0.1 \leq \alpha_0 \leq 0.5$ and $c_{min} = 0.05$ (when $k = k_{max}$) based on the problem complexity. Initial sensitivity study in this work showed that faster convergence and more stable search process is obtained when $\alpha_0 = 0.5$ and $c_{min} = 0.08$ for both well location and control optimization. The optimization process terminates after a predefined maximum number of iterations is reached.

Multisolution Optimization Framework

The developed optimization framework selects an ensemble of representative solutions from each optimization level to be optimized in the subsequent level. The aim is to select an ensemble of close-to-optimum solutions, with distinct differences in the decision parameters, from all the optimization iterations performed at each individual level. Such ensemble selection workflow is mathematically similar to the workflow used to select several representative reservoir model realizations from a pool of the possible ones generated due to the model uncertainty. By analogy, the control variables can be treated as an uncertainty while optimal solutions are the realizations. Then, a similar approach as the one by Sefat et al. (2016) can be employed to select an ensemble of representative realizations (optimal solutions) from each level, as explained below.

Selecting an Ensemble of Representative Solutions. The solutions with low objective function values or with high objective function values but with the decision variable values close to an optimum solution's already selected are not good for the representative ensemble of optimal solutions from each level. Hence, only the representative solutions with distinct difference in decision parameters are selected from the (p%) of the cases with top NPVs. The optimal value of p (p_{opt}) depends on two competing criteria: distinct dissimilarity of the selected solutions and proximity of the objective value of the selected cases to the maximum NPV. Selecting a large percentage of cases at each level ($p_{opt}\% \rightarrow all\ cases$) captures the maximum diversity between optimization scenarios. However, the selected cases do not all have the potential to achieve the close-to-optimum objective function values after next level of optimization, and therefore, their use only slows down the optimization speed. In our case, a sensitivity study showed that selecting top 20% (by NPV) solutions at each optimization level (i.e., $p_{opt} = 20\%$) showed the best performance in both sufficiently capturing the ensemble diversity yet showing a relatively fast optimization speed. Details of the sensitivity study are presented in the section "Tuning p_{opt} %."

Similarity/Dissimilarity Distance Measure. The similarity/dissimilarity between the selected solutions are measured as a pairwise distance between their corresponding control vectors. The control (variable) vectors are normalized into [0,1] domain using Eq. 2 to eliminate the impact of having control variables of different types and scales. Conventional Euclidean distance is then used to calculate the similarity/dissimilarity between the selected members of the ensemble of solutions at the well control optimization level [a similar approach was used by Sefat et al. (2016)]. Note that the conventional Euclidean distance of two identical solutions with the well names merely swapped, confusingly shows a nonzero distance (or dissimilarity) between them (Fig. 2a shows a two-well example). Hence, a modified measure is employed comparing distances between the reservoir grids with active wells irrespective of the well names (Fig. 2b shows a two-well example), as shown in Algorithm 1.

Algorithm 1—Pseudo-code for similarity/dissimilarity distance measurement between selected ensemble of well placement solutions

Assume ne_{well} is the number of members of the selected ensemble of well placement solutions. The reservoir model with D_X grids in x direction and D_Y grids in y direction could be represented by a $D_X \times D_Y$ binary matrix G, with 1 for elements where a well is located, and zero elsewhere. Hence, each solution is denoted by G_i , $i = 1, 2, \ldots, ne_{well}$ with N_{well} (number of wells) nonzero elements.

Do for i and, $i, j = 1, 2, \ldots, ne_{well}$ *and* $i \neq j$

- *For each nonzero element of* G_i $(G_i(m, n) = 1)$*, find the nearest* $G_j(m', n') = 1$ *(increase the radius of investigation around* $G_i(m, n)$ *until finding the first nonzero element of* G_j*).*
- *Compute the Euclidean distance between two nearest elements.*

$$d\left[G_i(m,n), G_j(m\prime, n')\right] = \sqrt{\left(G_i(m,n) - G_j(m',n)\right)^2 + \left(G_i(m,n) - G_j(m,n')\right)^2}$$

- *Compute the sum of Euclidean distances between all non-zero pairs of* G_i *and* G_j*.*

$$D(G_i, G_j) = \sum_{k=1}^{N_{well}} d\left[G_i(m_k, n_k), G_j\left(m'_k, n'_k\right)\right]$$

End do

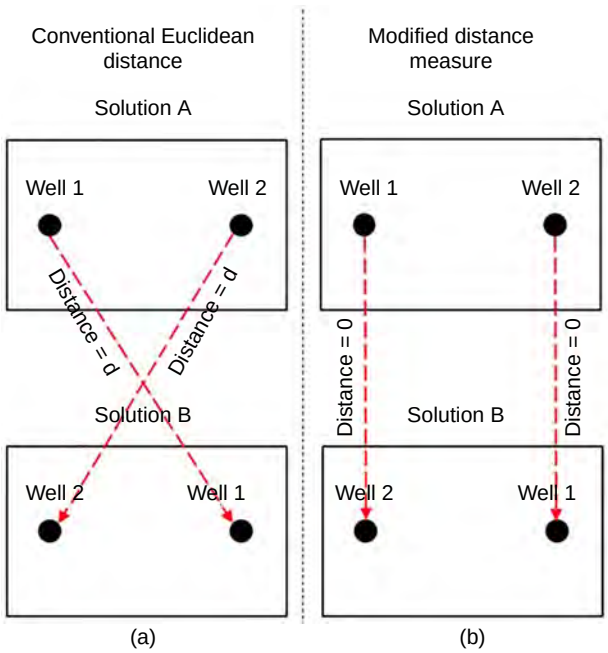

Fig. 2—A two-well example for (a) Conventional Euclidean distance measure based on well names. (b) Modified distance measure based on reservoir grid blocks with active well (irrespective of well names).

Multidimensional Scaling and K-Means Clustering. The similarity/dissimilarity distance measures described above are used to generate distance matrices of size $ne \times ne$, where ne is the ensemble size of the selected solutions at each optimization level. K-means clustering (Seber 2009) is employed in this study due to its conceptual simplicity and computational efficiency. However, the performance of K-means clustering is usually degraded when clustering high-dimensional data due to an increase in the number of variables during the clustering process (Tajunisha and Saravanan 2010; Sun et al. 2012). Hence, the direct use the original dataset (of size $ne \times ne$ in this study) in K-means clustering is not recommended. Following Caers et al. (2009), Wang et al. (2012), and Haghighat Sefat (2016), multidimensional scaling (MDS) (Borg and Groenen 2003) is employed to map the solutions into 2D space while preserving the characteristics of the data as much as possible. The choice of the projection into 2D space is validated by performing principal component analysis as explained in the results section. Hence, the relative distance between points in 2D space roughly represents dissimilarity of the solution scenarios in the original space. Moreover, the visualization of the 2D data points provides valuable insights into the characteristics of the search space as well as the clustering and optimization performance.

The objective is to use K-means clustering to group the projected solutions into a small number of clusters (N_c). Hence, the optimum number of clusters (N_{copt}) is identified by comparing the average silhouette values (Sefat et al. 2016) of all data points for different (N_c), where the maximum silhouette value shows the best clustering performance. A single, representative solution is then selected from each cluster, resulting in N_{copt} solutions as the representative solutions from that particular level of optimization, to be transferred to the next level.

Well Placement and Control Constraints. The maximum and minimum liquid production rates and water injection rates are considered as bound constraints during well control optimization. A minimum interwell distance constraint is enforced during well placement optimization using the penalty method similar to the one in Lu et al. (2017a). Previous studies (Bellout et al. 2012; Li and Jafarpour 2012; Li et al. 2013; Awotunde and Naranjo 2014; Lu et al. 2017a, Al-Ismael et al. 2018) use inequalities constraints to ensure wells are located within a rectangular domain inside irregular reservoir boundaries. This work accounts for irregular reservoir boundaries by generating a binary matrix with zero and one elements representing null and active reservoir grids, respectively. The well is moved to the nearest active grid if it appears outside the reservoir boundaries during location optimization (see Algorithm 2). **Fig. 3** shows the flow diagram of the multisolution framework with well placement and control settings as the optimization levels.

Algorithm 2—Pseudo-code accounting for irregular boundaries during well location optimization

Assume that binary matrix B corresponds to a reservoir top's model, where

$$B(i,j) = \begin{cases} 1, \textit{ if } (i,j) \textit{is an active grid of reservoir} \\ 0, \textit{ if } (i,j) \textit{is a grid outside of reservoir} \end{cases}$$

N_{well} denotes the number of wells, $B(i,j)_k$ represents an iteration of the location of well k.

Do for $k = 1, 2, \ldots, N_{well}$

- *If* $B(i,j)_k = 1$ then
  Well k is inside the reservoir boundaries.
- *If* $B(i,j)_k = 0$ then
  - *Find the nearest element of matrix B such that* $B(i',j') = 1$ *and* $d[B(i,j), B(i',j')] = \sqrt{(B(i,j) - B(i',j))^2 + (B(i,j) - B(i,j'))^2}$ *is minimum.*
  - *Replace* $B(i,j)$ *with* $B(i',j')$.

End do

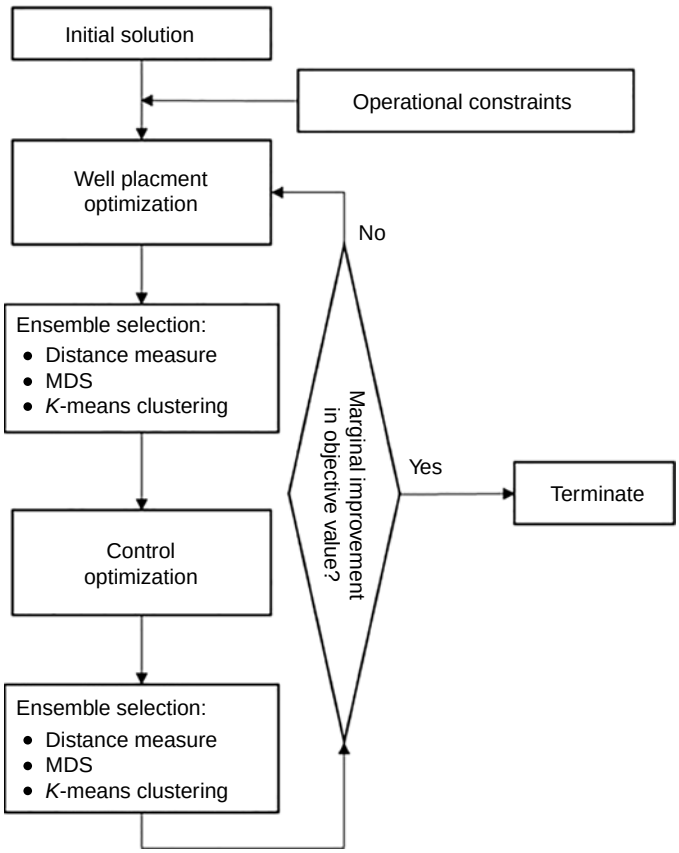

Fig. 3—Flow diagram of the proposed multisolution optimization framework.

Case Study 1—Brugge Model

Brugge is a publicly available benchmark reservoir model based on a North Sea field, consisting of $139 \times 48 \times 9$ grid blocks (total of 60,048 grid blocks of which approximately 45,000 are active) with a relatively heterogeneous permeability distribution (Chen et al. 2010). The original model consists of 20 producers and 10 injectors. Five vertical producers (named $P1$ to $P5$ in the original model) and five vertical injectors (named $I1, I3, I5, I7, I10$ in the original model) are kept from the original model in this work due to the limited computational resources. **Fig. 4** shows the top structure of the model with the base case well locations. More information on the reservoir rock and fluid properties of the Brugge model can be found in Peters et al. (2010). The objective function NPV (Eq. 1) is calculated using the economic parameters provided in **Table 1.** Three hundred iterations are performed at each optimization level to ensure

objective value convergence. Note that a single geological realization is considered in this work due to its being merely a proof-of-concept study; however, the developed framework can easily be applied to multiple realizations in a robust optimization problem to account for the geological uncertainty in the reservoir model, if required.

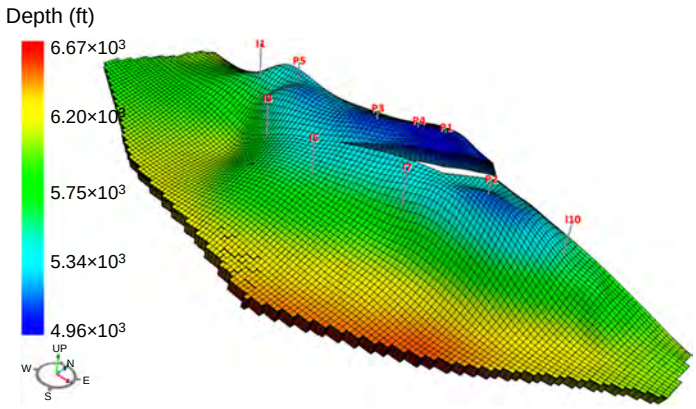

Fig. 4—Top structure of the Brugge model and initial well locations.

Parameter	Value
Oil price	50 USD/STB
Water production cost	6 USD/STB
Water injection cost	3 USD/STB
Discount rate	10 %/year

Table 1—Economic parameters for calculating the NPV.

Top (i, j) locations of the vertical wells are optimized during the stage of well location optimization over the set of $10 \times 2 = 20$ control variables. The producers are each controlled by its fixed, liquid production rate, while the injectors are each controlled by its fixed, water injection rate, both bounded between 0 and 5,000 STB/day. Moreover, the producers are shut when their water cut reaches 90% because after this WC value the well production is no longer profitable for the oil price and water cost values listed in Table 1. The 30 years of the field production period are divided into six control steps of equal duration (of 5 years) resulting in the total of $10 \times 6 = 60$ well production/injection control variables used in the well control optimization.

The NPV of the base case with nonoptimal well locations and fully open control settings is 2.111×10^9 USD, which was improved to 2.597×10^9 USD after the well location optimization level, as shown in **Fig. 5.** The top 20% NPV ($p_{opt} = 20$) of the well location optimization solutions are selected (i.e., 60 out 300 total iterations), and the dissimilarity matrix is generated using the modified distance measure (Algorithm 1). **Fig. 6** shows the projection of the selected solutions into 2D space using MDS Note that principal component analysis, performed on the dissimilarity matrix of the selected well placement solutions to corroborate the 2D mapping approach used, showed that the first two dimensions account for approximately 70% of the variance in the original dataset of $N_x = 20$ dimensions) in which each data point represents a well location solution with color showing the NPV. A reasonable degree of variability in the well location solutions is observed while the NPV among them changes within a relatively small range (2.597×10^9 – 2.559×10^9 USD). Fig. 6 also shows that there are solutions with different well locations but close NPVs, confirming that the search space is characterized by different local optima with close-to-optimum objective values.

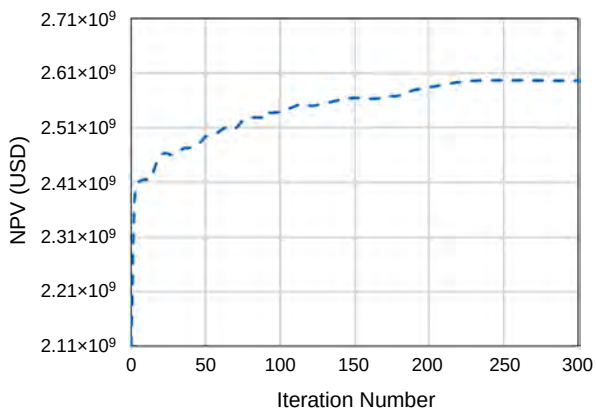

Fig. 5—Objective value during the well location optimization process for the Brugge model.

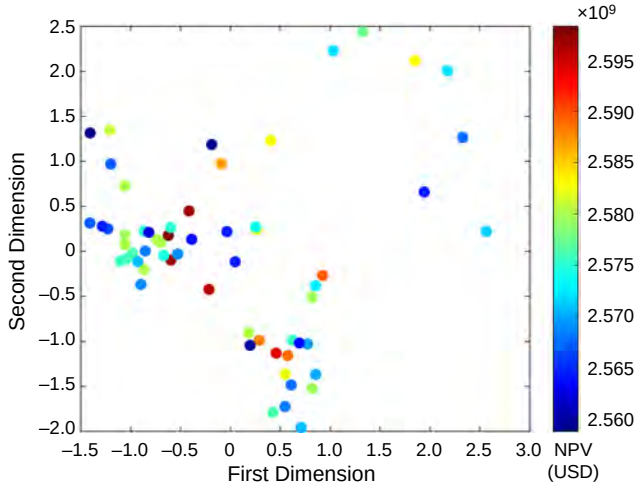

Fig. 6—Projection of 60 well location solutions into a 2D space using MDS (associated with their corresponding NPVs).

Fig. 7 shows the average silhouette values of all data points as a function of N_c. Here, the three-cluster set (the red point) is considered to be optimum providing a balance between computation time and clustering performance. **Fig. 8** shows results of the K-means clustering of selected well placement solutions in three groups. Selecting one representative solution from each cluster is a critical decision that needs to be made prior to the next level of optimization. Some previous works [e.g., Wang et al. (2012); Li and Durlofsky (2016); Sefat et al. (2016)] selected the member closest to the center. In this work, the solution with the maximum NPV in each cluster is selected as the representative of that cluster, which eventually leads to finding the (reasonably variable) solutions with the highest NPVs as per the objective of our study. The maximum NPV case (i.e., the optimal solution of the classic sequential approach) is automatically selected as one of the representatives. The representative well placement solutions (L_1, L_2, and L_3) are shown in **Fig. 9.**

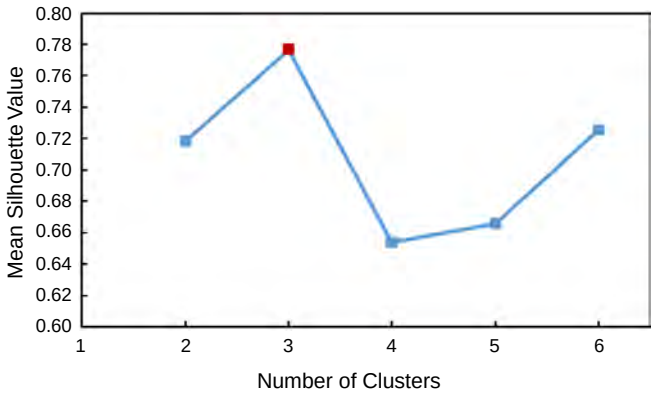

Fig. 7—Mean silhouette value of 60 well location solutions for different number of clusters.

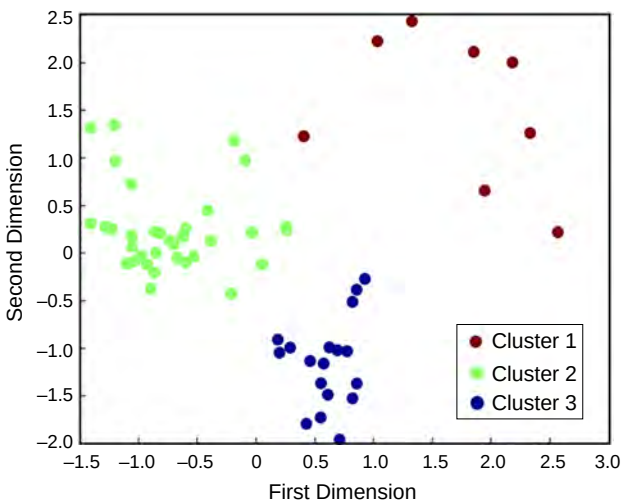

Fig. 8—K-means clustering for the ensemble of close-to-optimum well location solutions considering three clusters (N_c=3).

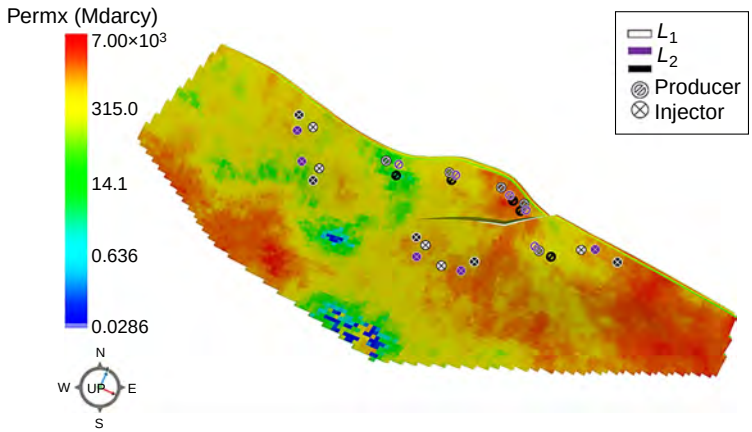

Fig. 9—Three optimal well locations' strategies L_1, L_2, and L_3 in the Brugge model with NPVs of 2.597×10^9 USD, 2.589×10^9USD, and 2.583×10^9USD, respectively.

The control settings of three optimal well locations are then individually optimized at the second optimization level. **Fig. 10** shows the control optimization process for each optimal well placement. A similar clustering approach is applied to the control solutions where an ensemble of representative solutions is selected from the top 20% (by NPV) of the cases. Conventional Euclidean distance is used to measure the dissimilarity between control scenarios followed by MDS to map them into 2D space **(Fig. 11).** Principal component analysis is individually performed for each of the three matrices of the selected control solutions obtained from well control optimization level, prior to MDS and K-means clustering. Results showed that the first two dimensions of each dissimilarity matrix preserve approximately 70% of the variance of their original data sets, similar to the well placement level. **Fig. 12** shows the average silhouette values analysis for each ensemble, suggesting $N_{copt} = 3$ for the scenarios with well placement strategies L_1 and L_3, and $N_{copt} = 5$ for the scenario with well placement strategy L_2. **Fig. 13** shows the K-means clustering based on the optimal number of clusters. The control scenario with the maximum NPV is selected from each cluster as the representative of that cluster, resulting in 11 optimal well control scenarios **(Fig. 14 and Fig. 15)** with three well placement strategies. A reasonable level of variability in the optimal controls is observed while NPV changes in a small range (2.921×10^9 – 2.977×10^9 USD), demonstrating that indeed there are different optimal controls with close-to-optimum objective values.

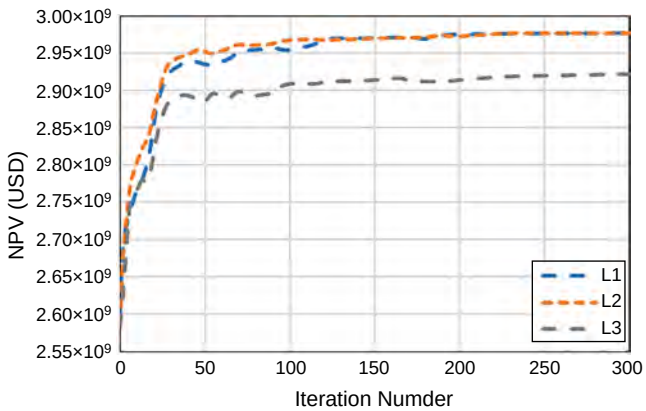

Fig. 10—Control optimization processes for three close-to-optimum well placement scenarios in Brugge model.

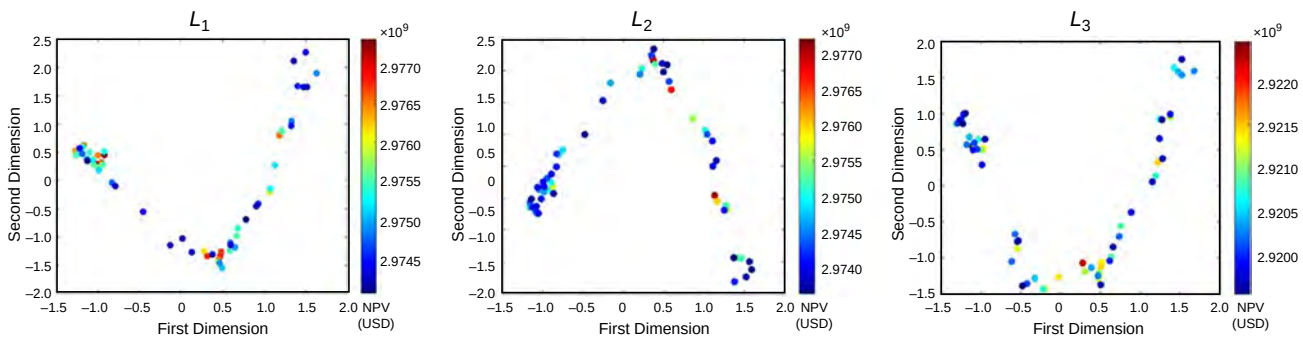

Fig. 11—Mapping of 60 well control solutions, attributed to L_1, L_2, and L_3 into a 2D space using MDS.

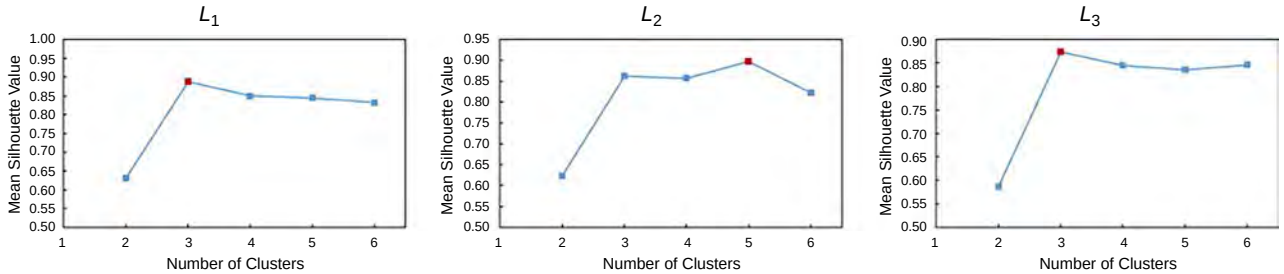

Fig. 12—Mean silhouette value of data points (ensemble of well control solutions based on L_1, L_2, and L_3) for different number of clusters in K-means.

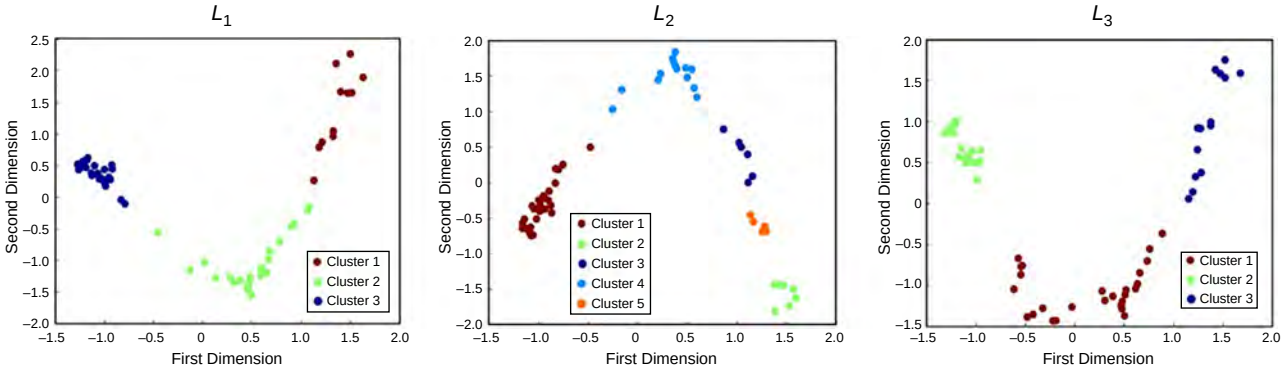

Fig. 13—K-means clustering for well control solutions (based on three well placement scenarios) considering the optimal number of clusters for each set of data points.

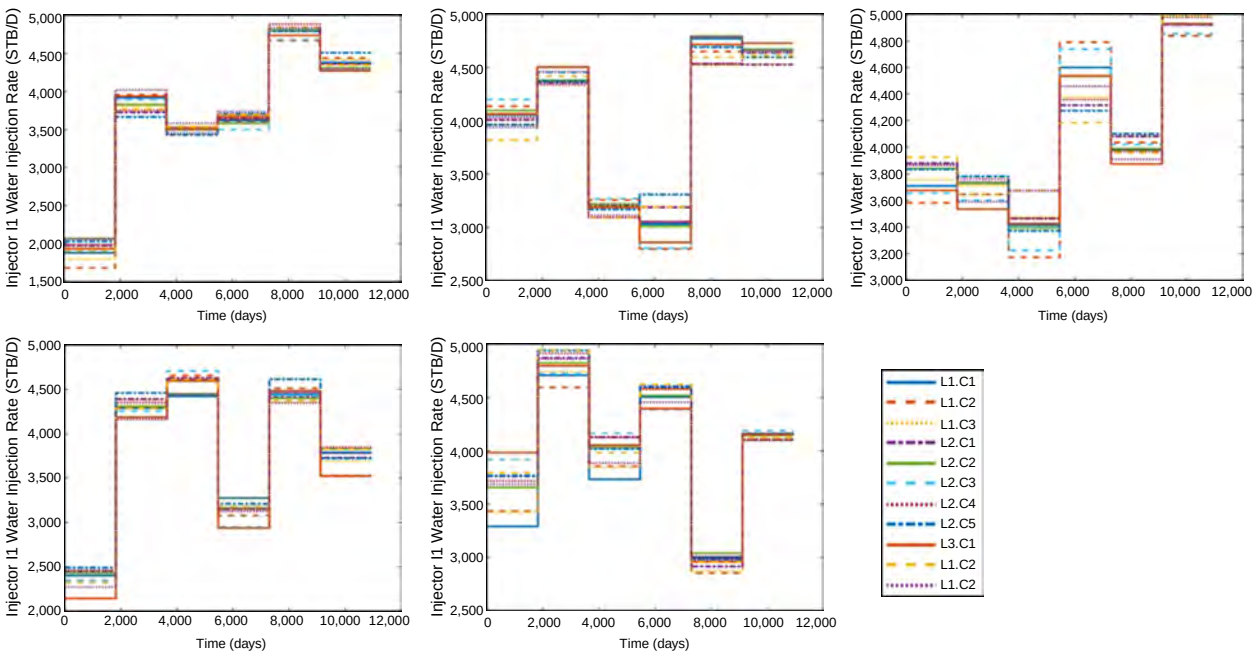

Fig. 14—The optimal water injection rates for the Brugge model obtained with multisolution framework.

The sequential optimization loop was then terminated because no further improvements in the objective value were obtained. **Table 2** compares the base case NPV with the selected three optimal well placement solutions and the results of the subsequent, best control settings scenarios for each of these well placement strategies. Although L_1 shows the maximum NPV at the well placement optimization level, L_2 shows higher further improvement due to the well control optimization (15.1%), illustrating that a suboptimal solution from the previous optimization level can approach and even outdo the optimal one at the next level. **Fig. 16** summarizes the tree structure of the developed multisolution framework, indicating the operational flexibility achieved by different field development and control scenarios with close-to-optimum NPVs. L_1C_1 and L_2C_1 are different field development and control scenarios with identical NPVs, while L_1C_2, L_2C_2, and L_2C_3 are other candidates with near globally optimum objective values. In this case study, three ensembles of well placement solution are selected, which results in performing two extra optimizations at the well control level as compared

to the traditional single-solution approach. While the main objective of the proposed multisolution framework is to deliver the much-needed operational flexibility to the operators (and this is indeed at a higher computation cost), further research to improve the computational efficiency of the framework will be useful.

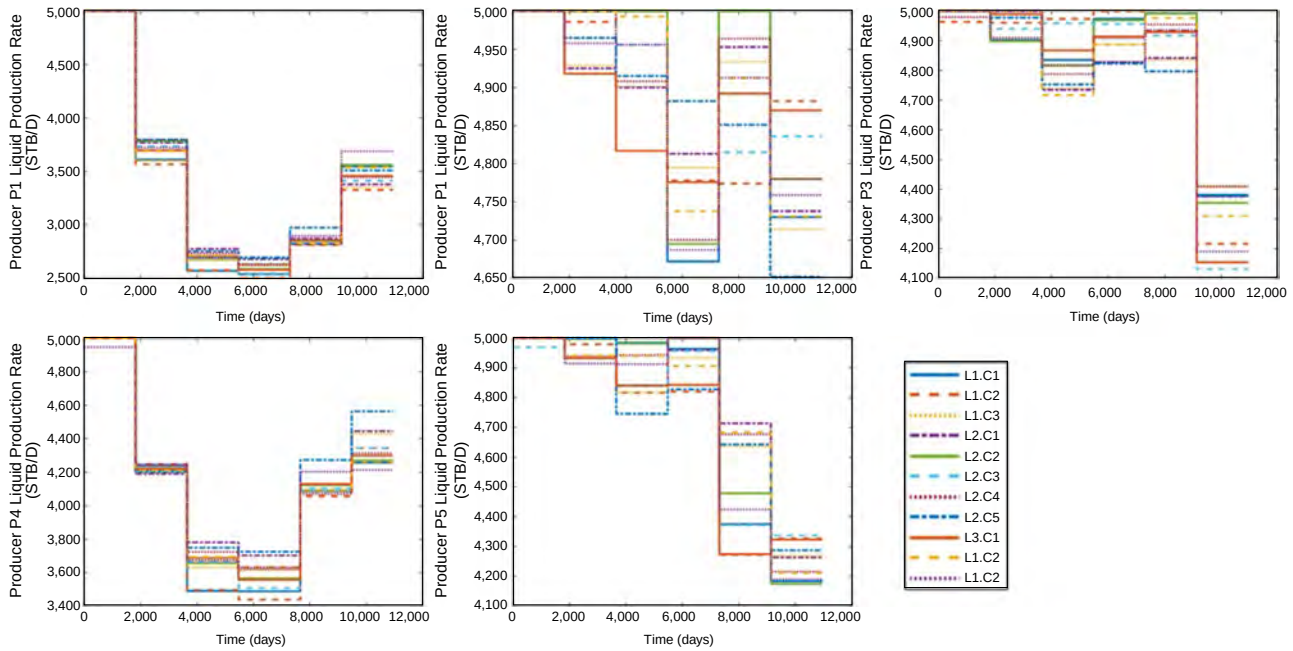

Fig. 15—The optimal liquid production (right) rates for the Brugge model obtained with multisolution framework.

Initial NPV (USD)		NPV after Well Placement Optimization (USD)	% Change	Maximum NPV after Further Well Control Optimization (USD)	% Change
2.111×10^9	L_1	2.597×10^9	23.2	2.977×10^9	14.6
	L_2	2.589×10^9	22.7	2.977×10^9	15.1
	L_3	2.583×10^9	22.3	2.922×10^9	13.2

Table 2—The summary of NPV values, before and after well placement and control settings optimization for Brugge model.

Note that the developed multisolution framework is compatible with different optimization algorithms and various other types of control variables (e.g., with zonal flow controls in smart wells, infill drilling options, etc.). However, the optimal percentage p_{opt}%, the optimization termination criteria, and the number of optimization cycles at these new conditions need to be determined afresh, as they rely on the available computational resources and the number of control variables.

Tuning $\mathbf{p_{opt}}$%. This section investigates the optimal value for p_{opt} in order to achieve the maximum diversity and the highest average NPV in an ensemble of selected solutions. The competition between these two criteria is examined by performing a sensitivity analysis on p_{opt}. The multisolution framework is repeated with p_{opt} values of 100%, 50%, 30%, and 5%, while the 20% option was already discussed in the case study section. The selected optimal solutions in each sensitivity are compared based on their pairwise similarity/dissimilarity in well placement scenarios. **Fig. 17** shows the 2D projection of the selected well locations for different p_{opt} values. Note that the solution with the maximum NPV (red circle) is naturally identical for all sensitivity cases. **Fig. 18** shows the average final NPV (after both well location and control optimization) of optimal solutions obtained with different p_{opt} percentages.

Relatively distinct solutions are obtained when $p_{opt} = 30, 50$, and 100 (Fig. 17); however, their average NPV is significantly lower than that of $p_{opt} = 5, 10$, and 20 (Fig. 18), indicating that the selected solutions with very low NPVs do not have the potential to achieve a close-to-optimum objective value. Though $p_{opt} = 10$ provides acceptable average NPV, it does not provide sufficiently different well placement scenarios as compared to the peer solutions. $p_{opt} = 5$ and 20 both provide relatively distinct solutions (one solution on the top right of the figures is identical in both cases) , while the average NPV obtained from $p_{opt} = 20$ is slightly higher than that of $p_{opt} = 5$, implying that those solutions selected from top $p_{opt} = 20$, though initially were lower ranked as compared to top 5% solutions, finally approached and exceeded the solutions selected from top $p_{opt} = 5$. Hence, $p_{opt} = 20$ is selected as the optimal value to select an ensemble of solutions during the optimization of the Brugge model. Note that because p_{opt} is a case-specific parameter, it might be different when other reservoir models and/or optimization algorithms are used. While tuning p_{opt} plays a crucial role in achieving diverse solutions, other remedies can also be applied to increase the diversity of well placement and control scenarios. For instance, using SPSA with different initial guesses (or seeds) at the well placement optimization level can potentially deliver multiple diverse field development scenarios. However, conducting multiple individual optimization cases could become computationally demanding. Further, separate research on optimal seeding and reducing the computational time of multiple parallel optimization cases could be useful. Another idea is to use global-search optimization algorithms, at least at early iterations to achieve diverse solutions. Metaheuristic algorithms, such as particle swarm optimization and genetic algorithms, can potentially deliver more diverse well placement solutions due

to their stochastic, population-based nature. In control optimization level, however, approximate-gradient-based algorithms are more preferable than metaheuristic algorithms due to the poor convergence of latter methods in problems with large number of control variables. Comparison of different optimization algorithms based on the diversity of the obtained solutions for each optimization level would provide insights into the optimal combination/configuration of the algorithms in the multisolution framework, though is beyond the scope of this paper.

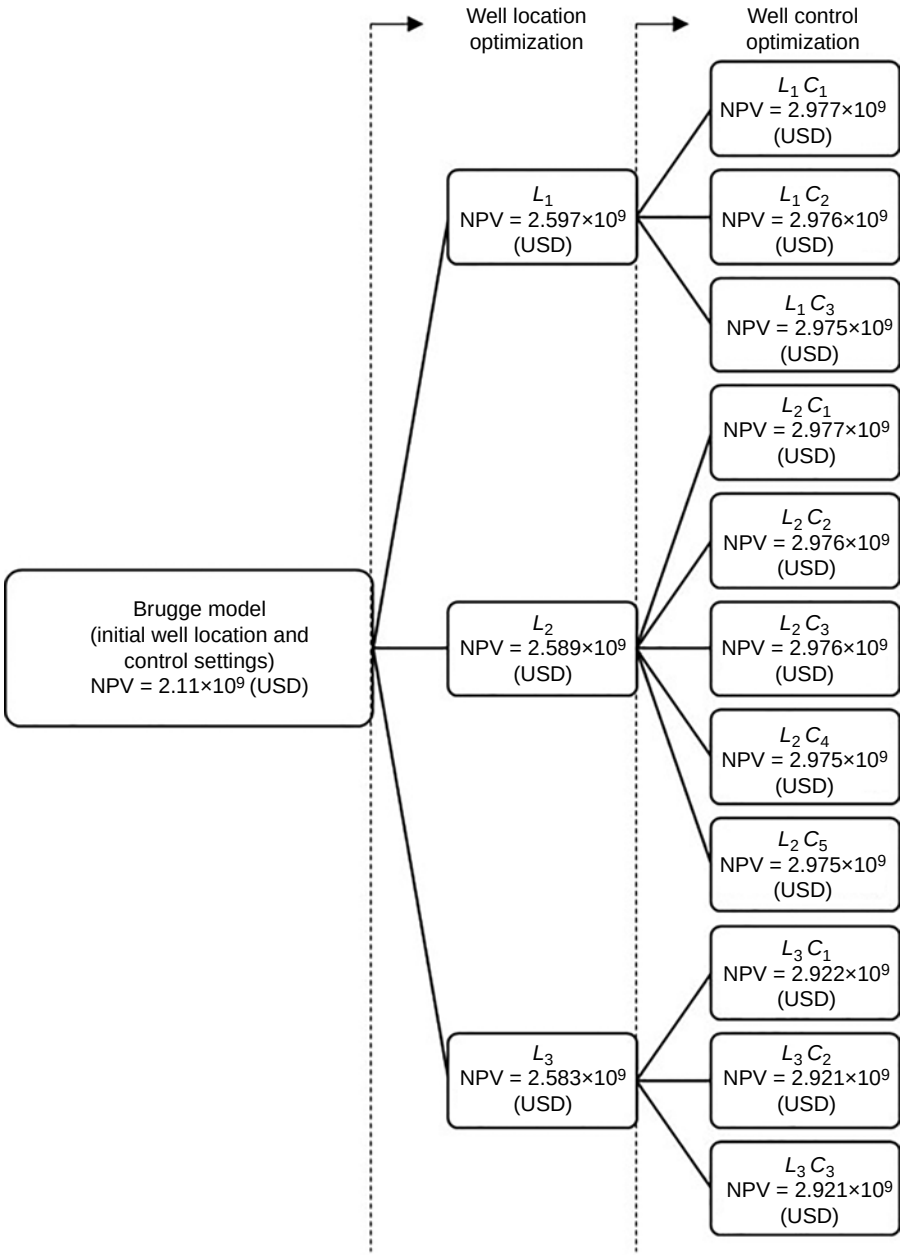

Fig. 16—Tree structure of multisolution optimization framework for the Brugge model.

Optimization Cycles. A significant aspect of the iterative sequential method is the desire to reach the global optimum. One method to improve the global convergence of stochastic approximation algorithms, such as SPSA, is the injection of additional noise terms into the perturbations in order to escape local optima (Maryak and Chin 1999). On the other hand, the iterative sequential method can use the premature termination of optimization levels to switch between the spaces of decision parameters to achieve the global optimum faster. However, an inappropriate selection of iteration numbers or termination criteria could result in suboptimal final solutions. In this section, the single-solution iterative sequential optimization approach is compared in two schemes:

- Multiple cycles of prematurely terminated optimization levels (iSeq-1) (a cycle here means level 1 optimization of the well locations followed by level 2 optimization of the well controls)
- Fewer cycles but with substantially iterated optimization levels (iSeq-2)

The maximum number of iterations for iSeq-1 is set to 50 and 30 for well placement and control settings optimization levels, respectively, while iSeq-2 is performed with 100 iterations for both optimization levels. The initial point, model properties, algorithm settings, constraints, and the order of optimization levels (one iteration of well placement is followed by an iteration of well control settings) in both schemes are identical.

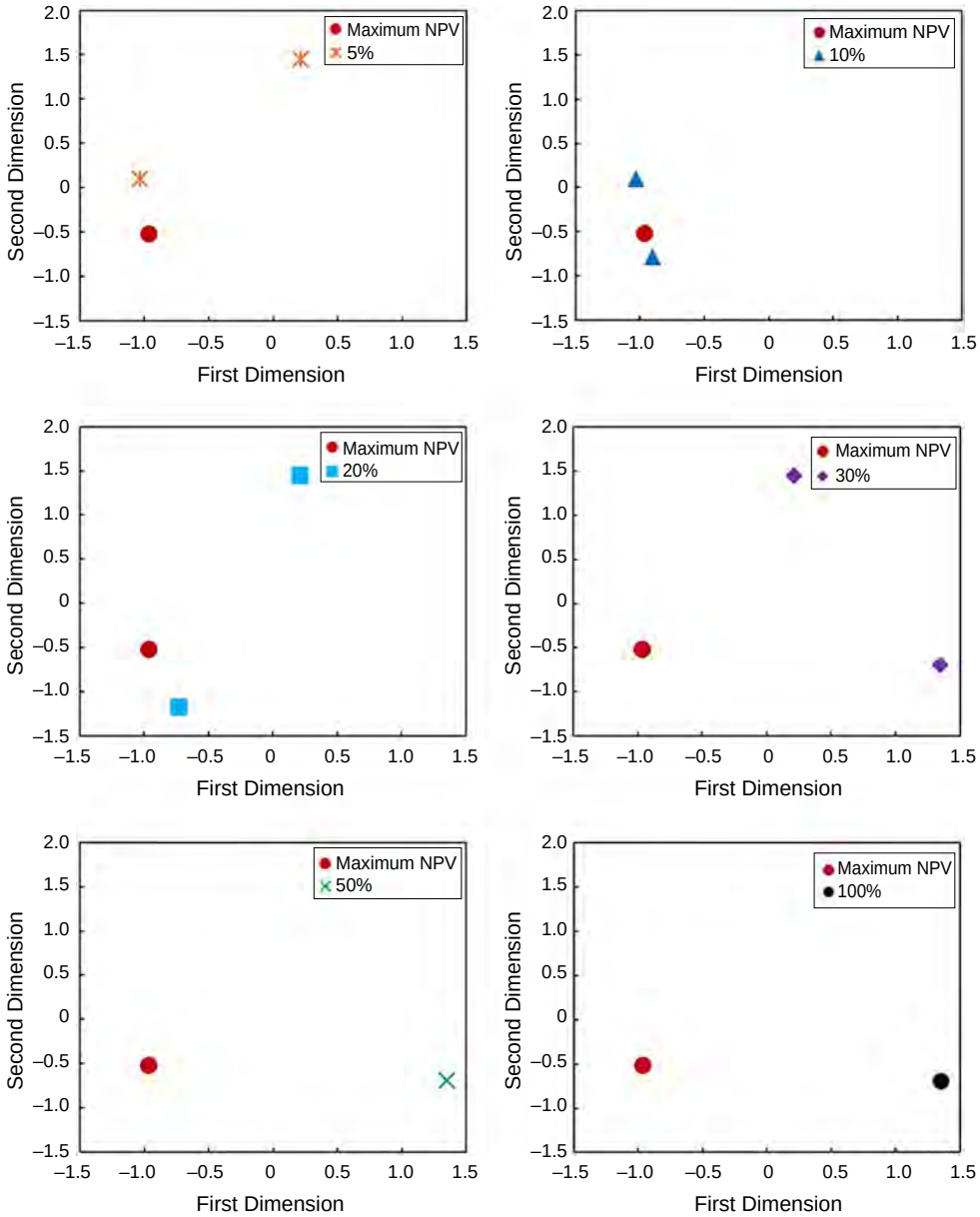

Fig. 17—2D representation of optimal well location solutions for different p_{opt} percentages.

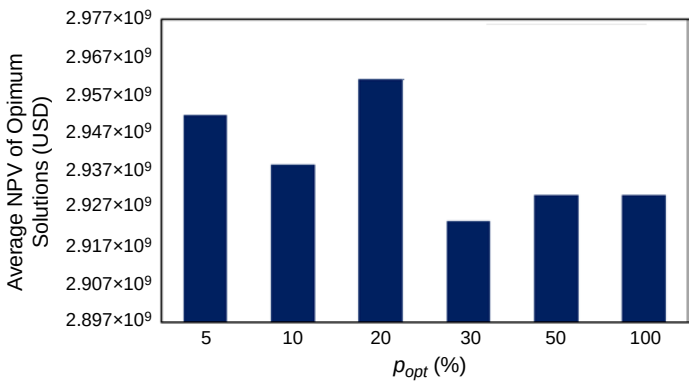

Fig. 18—Average NPV of optimal solutions for different p_{opt} percentages.

Fig. 19 shows the NPV as a function of iterations in iSeq-1 and iSeq-2 schemes. The iSeq-1 was terminated after the third go at the well location optimization level was finished [i.e., there were a total of $2 \times (50 + 30) + 50 = 210$ iterations], while the iSeq-2 was stopped after a single cycle (i.e., total of $2 \times 100 = 200$ iterations). Thus, both methods have had a similar number of iterations and computation time.

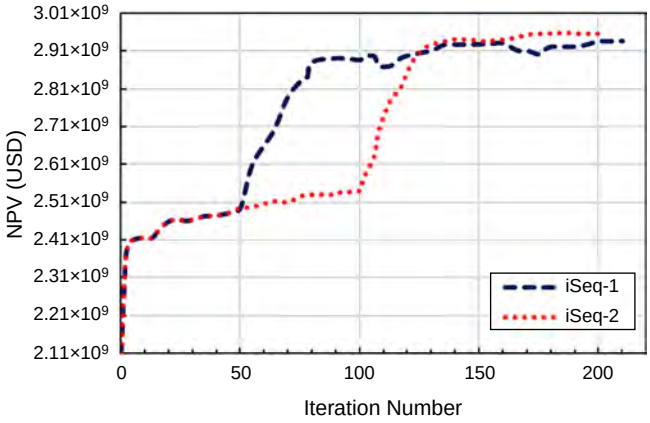

Fig. 19—Comparison of the NPV vs. number of iterations for the Brugge model using iSeq-1 and iSeq-2 schemes.

The comparison between two schemes shows that iSeq-2 also provides a similar (slightly higher in this particular case) improvement in the objective value as compared to iSeq-1 (Fig. 19). Using iSeq-1 approach, with a multisolution optimization framework, significantly increases the computation cost, as the number of branches of the tree structure (e.g., Fig. 16) increases exponentially with a larger number of cycles. Hence, it is preferred to perform minimum number of optimization cycles with higher number of iterations at each level (i.e., iSeq-2). The computation time can also be reduced by using the optimal solution of the case with the highest NPV as the initial starting point for the remaining optimization cases in the same level. This significantly improves the computational efficiency of the framework by speeding up the convergence to optimal solution, especially at the well control level in which lower diversity of selectable solutions is generally accepted due to the more flexible nature of the well control operations.

Case Study 2—Egg Model

The Egg reservoir model is a 3D channelized benchmark case study consisting of $60 \times 60 \times 7$ grid blocks, of which 18,553 are active. The model contains eight injectors and four producers. **Fig. 20** shows the horizontal permeability for a single geological realization of the field and the base case well locations. Detailed information on the reservoir rock and fluid properties of the Egg model can be found in (Jansen et al. 2014). The objective function NPV (Eq. 1) is calculated using the economic parameters provided in Table 1. Fifty and 100 iterations are performed at the well placement and the control optimization levels, respectively. A lower number of iterations was found to be sufficient for the well placement optimization level due to the lower number of active grid blocks as compared to the Brugge model. Top (i, j) locations of the vertical wells are optimized during well location optimization resulting in $12 \times 2 = 24$ control variables. The four producers are operated at the constant BHP of 5,727 psi, and they are shut in when their water cut exceeds 90%. The eight injectors are each controlled by its water injection rate, varied between 0 and 500 STB/day. The 10 years of the field production period are divided into 10 control steps (of 1 year each) resulting in the total of $8 \times 10 = 80$ well injection control variables at the well control optimization level.

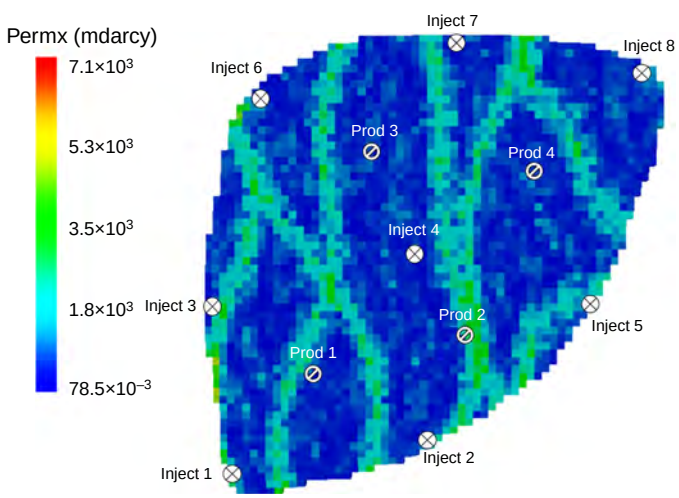

Fig. 20—Permeability field and the base case well locations of the Egg model.

The NPV of the base case, with nonoptimal well locations and fully open control settings (maximum water injection rate), is 1.49×10^7 USD, which was improved to 1.78×10^7 USD after optimizing the well locations. In this example, selecting the top 30% (by NPV) solutions at each optimization level (i.e., $p_{opt} = 30\%$) delivered the best performance (when compared to $p = 5$, 10, 30, 50, and 100, similar to the previous case study) in both sufficiently capturing the ensemble diversity and showing a relatively high average objective value. The desire to capture enough diversity from the well placement optimization iterations in a more limited search space of the Egg model with the lower number of active grid blocks has resulted in the higher p_{opt} value in this case, as compared to the case study 1 (in which it was 20%) (note that well placement optimization for Brugge and Egg models are each performed within

$139 \times 48 = 6{,}672$ and $60 \times 60 = 3{,}600$ grid blocks, respectively). The dissimilarity matrix is then generated (using the modified distance measure as per Algorithm 1), followed by its projection into 2D space using MDS. The optimum number of clusters is identified as 2 ($N_{copt} = 2$) after the average silhouette value analysis. K-means clustering is then performed, followed by selecting the solution with the maximum NPV in each cluster as the representative of that cluster. **Fig. 21** shows the representative well placement solutions ($L_1$and L_2). A relatively high degree of variability in the well location solutions can be observed while the NPV among them changes within a very small range (1.78×10^7 USD for $L_1$and 1.77×10^7 USD for L_2).

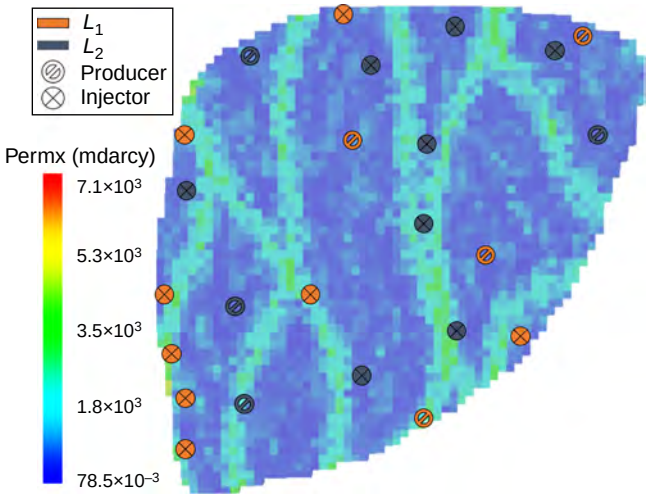

Fig. 21—Two optimal well locations' strategies $L_1$and L_2 in the Egg model with NPVs of 1.78×10^7 USD and 1.77×10^7USD, respectively.

The wells' water injection rates for the two optimal well location scenarios are then individually optimized at the second optimization level with 100 iterations for each case. A similar clustering approach is applied to the control solutions where an ensemble of representative solutions is selected from the top 30% (by NPV) of the cases. The conventional Euclidean distance is used to measure the dissimilarity between control scenarios followed by MDS to map them into 2D space. The optimum number of clusters were identified as 3 ($N_{copt} = 3$) after carrying out the average silhouette value analysis for both scenarios with well placement strategies L_1 and L_2. K-means clustering is then performed based on the optimal number of clusters followed by selecting the control scenario with the maximum NPV from each cluster as the representative of that cluster. This results in six optimal well control scenarios **(Fig. 22)** with two well placement strategies. A reasonable level of variability in the optimal controls is observed while NPV changes in a small range ($2.030\times10^7 - 1.961\times10^9$ USD), demonstrating that there are different optimal controls with close-to-optimum objective values.

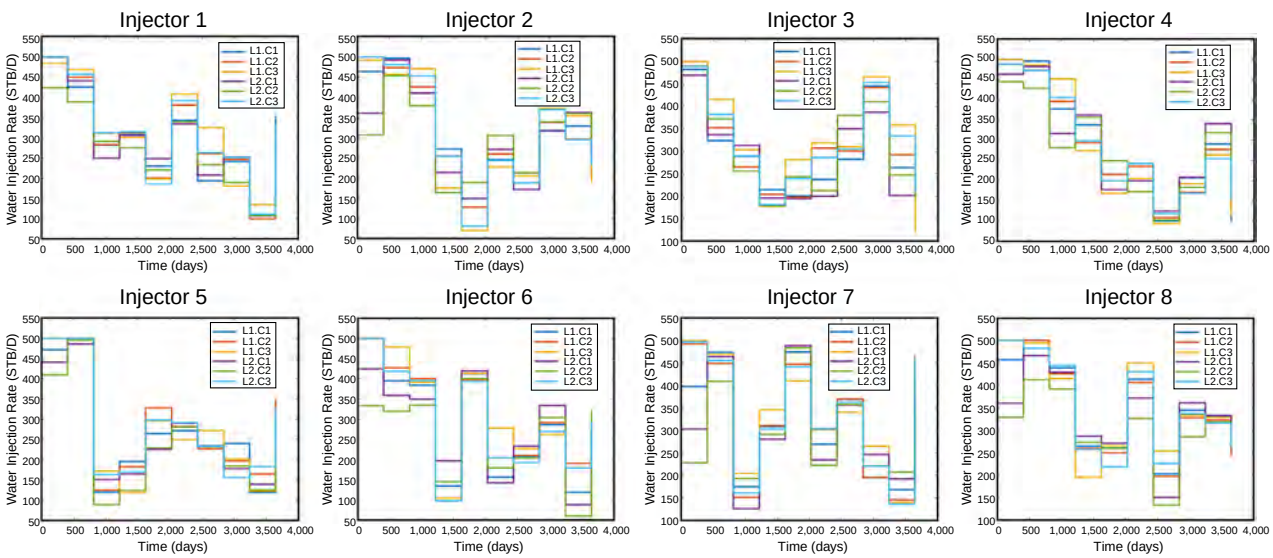

Fig. 22—The optimal water injection rates for the Egg model obtained with the multisolution framework.

The sequential optimization loop was then terminated since no further improvements in the objective value was obtained for all field development and control scenarios. **Table 3** compares the base case NPV with the selected two optimal well placement solutions, and the results of the subsequent, best control settings scenarios for each of these well placement strategies. **Fig. 23** summarizes the results of the developed multisolution optimization framework applied to the Egg model using a tree structure. Although L_1 provides the maximum NPV at the well placement optimization level with base-case control scenario, L_2 shows higher ultimate NPV after the well

control optimization, demonstrating that a suboptimal solution from the previous optimization level can approach and even outdo the optimal one at the next level. These results are in line with the case study 1, showing the value of the developed multisolution optimization framework to deliver operational flexibility as well as a more efficient exploration of the search space.

Initial NPV (USD)		NPV after Well Placement Optimization (USD)	% Change	Maximum NPV after Further Well Control Optimization (USD)	% Change
1.49×10^7	L_1	1.78×10^7	19.5	1.96×10^7	10.1
	L_2	1.77×10^7	18.8	2.03×10^7	14.7

Table 3—The summary of NPV values, before and after well placement and control settings optimization for Egg model.

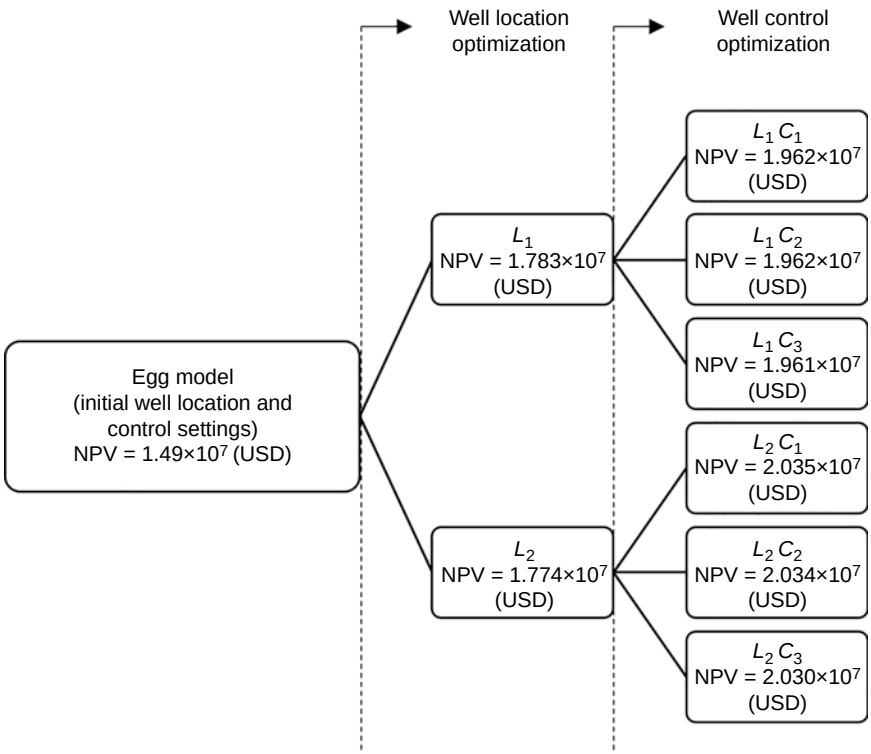

Fig. 23—Tree structure of multisolution optimization framework for the Egg model.

Conclusions

Offering optimal yet flexible field development and control decisions to ensure against unexpected operational constraints is an ambitious and highly demanded objective in reservoir engineering. This study presented a multisolution optimization framework that provides multiple optimal solutions by efficiently exploring the decision variables' search space. A systematic clustering procedure was developed to select an ensemble of distinctly different, field development scenarios with close-to-optimum objective values. The SPSA algorithm was employed in a multilevel iterative sequential approach to find optimal well locations and control settings. However, the developed framework is compatible with other optimization algorithms as well. In addition to the constraints on liquid production and water injection rates, a minimum well spacing and a modified procedure of respecting irregular reservoir boundaries were considered within the optimization procedure. The proposed framework has been tested on two benchmark case studies, known as Brugge and Egg models. Multiple optimal field development and control solutions with close-to-optimum objective values but different control variables were obtained. The algorithm tuning parameters were also found, justified, and published to ease implementation of our approach by reservoir engineering teams, where appropriate. The study results demonstrate that suboptimal solutions from an early optimization level can approach and even outdo the optimal one at the subsequent optimization levels, highlighting the advantage of the here-developed multisolution framework in order to provide the operational flexibility in field optimization problems. The number of optimization runs depends on the optimization cycles and the number of near-optimal solutions selected at each optimization level; hence, one of the objectives of this study was to identify the best combination of these two parameters to reduce the total number of simulation runs required by performing minimum number of optimization cycles with higher number of iterations at each level.

Acknowledgments

We thank the sponsors of the "Value from Advanced Wells II (VAWE II)" Joint Industry Project at Heriot-Watt University for providing financial support and Schlumberger for allowing academic access to their software.

References

Al-Ismael, M., Awotunde, A., Al-Yousef, H. et al. 2018. A Well Placement Optimization Constrained to Regional Pressure Balance. Paper presented at the SPE Europec Featured at 80th EAGE Conference and Exhibition, Copenhagen, Denmark, 11–14 June. SPE-190788-MS. https://doi.org/10.2118/190788-MS.

Almeida, L. F., Vellasco, M. M., and Pacheco, M. A. 2010. Optimization System for Valve Control in Intelligent Wells under Uncertainties. *J Pet Sci Eng* **73** (1–2): 129–140. https://doi.org/10.1016/j.petrol.2010.05.013.

Awotunde, A. A. and Naranjo, C. 2014. Well Placement Optimization Constrained to Minimum Well Spacing. Paper presented at the SPE Latin America and Caribbean Petroleum Engineering Conference, Maracaibo, Venezuela, 21–23 May. SPE-169272-MS. https://doi.org/10.2118/169272-MS.

Bangerth, W., Klie, H., Wheeler, M. F. et al. 2006. On Optimization Algorithms for the Reservoir Oil Well Placement Problem. *Comput Geosci* **10** (3): 303–319. https://doi.org/10.1007/s10596-006-9025-7.

Bellout, M. C., Ciaurri, D. E., Durlofsky, L. J. et al. 2012. Joint Optimization of Oil Well Placement and Controls. *Comput Geosci* **16** (4): 1061–1079. https://doi.org/10.1007/s10596-012-9303-5.

Borg, I. and Groenen, P. 2003. Modern Multidimensional Scaling: Theory and Applications. *J Educ Meas* **40** (3): 277–280. https://doi.org/10.1007/s10596-012-9303-5.

Brouwer, D. R. and Jansen, J. D. 2002. Dynamic Optimization of Water Flooding with Smart Wells Using Optimal Control Theory. Paper presented at the European Petroleum Conference, Aberdeen, Scotland, United Kingdom, 29–31 October. SPE-78278-MS. https://doi.org/10.2118/78278-MS.

Bukshtynov, V., Volkov, O., Durlofsky, L. J. et al. 2015. Comprehensive Framework for Gradient-Based Optimization in Closed-Loop Reservoir Management. *Comput Geosci* **19** (4): 877–897. https://doi.org/10.1007/s10596-015-9496-5.

Caers, J., Park, K., and Scheidt, C. 2009. Modeling Uncertainty in Metric Space. Paper presented at the International Association of Mathematical Geology Meeting, Stanford University, Stanford, California, USA.

Chen, C., Wang, Y., Li, G. et al. 2010. Closed-Loop Reservoir Management on the Brugge Test Case. *Comput Geosci* **14** (4): 691–703. https://doi.org/10.1007/s10596-010-9181-7.

Chen, Y., Oliver, D. S., and Zhang, D. 2009. Efficient Ensemble-Based Closed-Loop Production Optimization. *SPE J*. **14** (04): 634–645. SPE-112873-PA. https://doi.org/10.2118/112873-PA.

Ciaurri, D. E., Mukerji, T., and Durlofsky, L. J. 2011. Derivative-Free Optimization for Oil Field Operations. In *Computational Optimization and Applications in Engineering and Industry*, eds. X. S. Yang and S. Koziel, Vol. 359, 19–55. Berlin, Heidelberg, Germany: Springer.

Eberhart, R. and Kennedy, J. 1995. A New Optimizer Using Particle Swarm Theory. Paper presented at the Sixth International Symposium on Micro Machine and Human Science, Nagoya, Japan, 4–6 October.

Fonseca, R. R.-M., Chen, B., Jansen, J. D. et al. 2017. A Stochastic Simplex Approximate Gradient (StoSAG) for Optimization under Uncertainty. *Int J Num Meth Eng* **109** (13): 1756–1776. https://doi.org/10.1002/nme.5342.

Fonseca, R. M., Leeuwenburgh, O., Van den Hof, P. M. J. et al. 2014. Ensemble-Based Hierarchical Multi-Objective Production Optimization of Smart Wells. *Comput Geosci* **18** (3–4): 449–461. https://doi.org/10.1007/s10596-013-9399-2.

Forouzanfar, F., Poquioma, W. E., and Reynolds, A. C. 2016. Simultaneous and Sequential Estimation of Optimal Placement and Controls of Wells with a Covariance Matrix Adaptation Algorithm. *SPE J*. **21** (02): 501–521. SPE-173256-PA. https://doi.org/10.2118/173256-PA.

Haghighat Sefat, M. 2016. *Proactive Optimisation of Intelligent Wells under Uncertainty*. PhD dissertation, Heriot-Watt University, Edinburgh, Scotland, United Kingdom.

Holland, J. H. 1992. *Adaptation in Natural and Artificial Systems: An Introductory Analysis with Applications to Biology, Control, and Artificial Intelligence*. Cambridge, Massachusetts, USA: MIT Press.

Isebor, O. J., Durlofsky, L. J., and Ciaurri, D. E. 2014. A Derivative-Free Methodology with Local and Global Search for the Constrained Joint Optimization of Well Locations and Controls. *Comput Geosci* **18** (3–4): 463–482. https://doi.org/10.1007/s10596-013-9383-x.

Isebor, O. J., Echeverría Ciaurri, D., and Durlofsky, L. J. 2014. Generalized Field-Development Optimization with Derivative-Free Procedures. *SPE J*. **19** (05): 891–908. SPE-163631-PA. https://doi.org/10.2118/163631-PA.

Jansen, J.-D., Fonseca, R.-M., Kahrobaei, S. et al. 2014. The Egg Model—A Geological Ensemble for Reservoir Simulation. *Geosci Data J* **1** (2): 192–195. https://doi.org/10.1002/gdj3.21.

Kraaijevanger, J. F. B. M., Egberts, P. J. P., Valstar, J. R. et al. 2007. Optimal Waterflood Design Using the Adjoint Method. Paper presented at the SPE Reservoir Simulation Symposium, Houston, Texas, USA, 26–28 February. SPE-105764-MS. https://doi.org/10.2118/105764-MS.

Li, G. and Reynolds, A. C. 2011. Uncertainty Quantification of Reservoir Performance Predictions Using a Stochastic Optimization Algorithm. *Comput Geosci* **15** (3): 451–462. https://doi.org/10.1007/s10596-010-9214-2.

Li, H. and Durlofsky, L. J. 2016. Local–Global Upscaling for Compositional Subsurface Flow Simulation. *Transp Porous Med* **111** (3): 701–730. https://doi.org/10.1007/s11242-015-0621-7.

Li, L. and Jafarpour, B. 2012. A Variable-Control Well Placement Optimization for Improved Reservoir Development. *Comput Geosci* **16** (4): 871–889. https://doi.org/10.1007/s10596-012-9292-4.

Li, L., Jafarpour, B., and Mohammad-Khaninezhad, M. R. 2013. A Simultaneous Perturbation Stochastic Approximation Algorithm for Coupled Well Placement and Control Optimization under Geologic Uncertainty. *Comput Geosci* **17** (1): 167–188. https://doi.org/10.1007/s10596-012-9323-1.

Lu, R., Forouzanfar, F. and Reynolds, A. C. 2017a. Bi-Objective Optimization of Well Placement and Controls Using StoSAG. Paper presented at the SPE Reservoir Simulation Conference, Montgomery, Texas, USA, 20–22 February. SPE-182705-MS. https://doi.org/10.2118/182705-MS.

Lu, R., Forouzanfar, F., and Reynolds, A. C. 2017b. An Efficient Adaptive Algorithm for Robust Control Optimization Using StoSAG. *J Pet Sci Eng* **159**: 314–330. https://doi.org/10.1016/j.petrol.2017.09.002.

Lu, R. and Reynolds, A. C. 2019. Joint Optimization of Well Locations, Types, Drilling Order and Controls Given a Set of Potential Drilling Paths. Paper presented at the SPE Reservoir Simulation Conference, Galveston, Texas, USA, 10–11 April. SPE-193885-MS. https://doi.org/10.2118/193885-MS.

Maryak, J. L. and Chin, D. C. 1999. Efficient Global Optimization Using SPSA. Paper presented at the American Control Conference, San Diego, California, USA, 2–4 June, Cat No 99CH36251.

Onwunalu, J. E. and Durlofsky, L. J. 2010. Application of a Particle Swarm Optimization Algorithm for Determining Optimum Well Location and Type. *Comput Geosci* **14** (1): 183–198. https://doi.org/10.1007/s10596-009-9142-1.

Panahli, C. 2017. *Implementation of Particle Swarm Optimization Algorithm within FieldOpt Optimization Framework-Application of the Algorithm to Well Placement Optimization*. Master's thesis, Norwegian University of Science and Technology, Trondheim, Norway.

Peters, L., Arts, R., Brouwer, G. et al. 2010. Results of the Brugge Benchmark Study for Flooding Optimization and History Matching. *SPE Res Eval & Eng* **13** (03): 391–405. SPE-119094-PA. https://doi.org/10.2118/119094-PA.

Sarma, P., Aziz, K., and Durlofsky, L. J. 2005. Implementation of Adjoint Solution for Optimal Control of Smart Wells. Paper presented at the SPE Reservoir Simulation Symposium, The Woodlands, Texas, USA, 31 January–2 February. SPE-92864-MS. https://doi.org/10.2118/92864-MS.

Schlumberger. 2017. *ECLIPSE® User Manual*. Houston, Texas, USA: Schlumberger.

Seber, G. A. 2009. *Multivariate Observations*, Vol. 252. Hoboken, New Jersey, USA: John Wiley & Sons.

Sefat, M. H., Elsheikh, A. H., Muradov, K. M. et al. 2016. Reservoir Uncertainty Tolerant, Proactive Control of Intelligent Wells. *Comput Geosci* **20** (3): 655–676. https://doi.org/10.1007/s10596-015-9513-8.

Shirangi, M. G., Volkov, O., and Durlofsky, L. J. 2018. Joint Optimization of Economic Project Life and Well Controls. *SPE J*. **23** (02): 482–497. SPE-182642-PA. https://doi.org/10.2118/182642-PA.

Spall, J. C. 1992. Multivariate Stochastic Approximation Using a Simultaneous Perturbation Gradient Approximation. *IEEE Trans Automat Contr* **37** (3): 332–341. https://doi.org/10.1109/9.119632.

Spall, J. C. 1998. Implementation of the Simultaneous Perturbation Algorithm for Stochastic Optimization. *IEEE T Aero Elec Sys* **34** (3): 817–823. https://doi.org/10.1109/7.705889.

Stoisits, R. F., Crawford, K. D., MacAllister, D. J. et al. 2001. Petroleum Production Optimization Utilizing Adaptive Network and Genetic Algorithm Techniques. *US Patent No. 6,236,894B1*.

Sun, W., Wang, J., and Fang, Y. 2012. Regularized k-Means Clustering of High-Dimensional Data and Its Asymptotic Consistency. *Electron J Stat* **6** (0): 148–167. https://doi.org/10.1214/12-EJS668.

Tajunisha, N. and Saravanan, V. 2010. An Increased Performance of Clustering High Dimensional Data Using Principal Component Analysis. Paper presented at the First International Conference on Integrated Intelligent Computing, Bangalore, India, 5–7 August.

Tavallali, M. S., Bakhtazma, F., Meymandpour, A. et al. 2018. Optimal Drilling Planning by considering the Subsurface Dynamics—Combing the Flexibilities of Modeling and a Reservoir Simulator. *Ind Eng Chem Res* **57** (48): 16367–16378. https://doi.org/10.1021/acs.iecr.8b00800.

Tavallali, M. S., Karimi, I. A., Teo, K. M. et al. 2013. Optimal Producer Well Placement and Production Planning in an Oil Reservoir. *Comput Chem Eng* **55**: 109–125. https://doi.org/10.1016/j.compchemeng.2013.04.002.

Tsou, D. and MacNish, C. 2003. Adaptive Particle Swarm Optimisation for High-Dimensional Highly Convex Search Spaces. Paper presented at the Congress on Evolutionary Computation (CEC'03), Canberra, Australia, 8–12 December, 783–789.

Van Essen, G., Van den Hof, P., and Jansen, J.-D. 2011. Hierarchical Long-Term and Short-Term Production Optimization. *SPE J*. **16** (01): 191–199. SPE-124332-PA. https://doi.org/10.2118/124332-PA.

Wang, H., Echeverría-Ciaurri, D., Durlofsky, L. et al. 2012. Optimal Well Placement under Uncertainty Using a Retrospective Optimization Framework. *SPE J*. **17** (01): 112–121. SPE-141950-PA. https://doi.org/10.2118/141950-PA.

Wang, P., Litvak, M., and Aziz, K. 2002. Optimization of Production Operations in Petroleum Fields. Paper presented at the SPE Annual Technical Conference and Exhibition, San Antonio, Texas, USA, 29 September–2 October. SPE-77658-MS. https://doi.org/10.2118/77658-MS.

Wang, X., Haynes, R. D., He, Y. et al. 2019. Well Control Optimization Using Derivative-Free Algorithms and a Multiscale Approach. *Comput Chem Eng* **123**: 12–33. https://doi.org/10.1016/j.compchemeng.2018.12.004.

Zingg, D. W., Nemec, M., and Pulliam, T. H. 2008. A Comparative Evaluation of Genetic and Gradient-Based Algorithms Applied to Aerodynamic Optimization. *Eur J Comput Mech* **17** (1–2): 103–126. https://doi.org/10.3166/remn.17.103-126.